

# Waveguide Optimization for a 9.0 $\mu\text{m}$ GaAs-Based Quantum Cascade Laser\*

Li Lu, Liu Fengqi<sup>†</sup>, Shao Ye, Liu Junqi, and Wang Zhanguo

(Key Laboratory of Semiconductor Material Science, Institute of Semiconductors, Chinese Academy of Sciences, Beijing 100083, China)

**Abstract:** Improved waveguide designs for 9.0 $\mu\text{m}$  GaAs-based quantum cascade laser (QCL) structures are presented. Modal losses and confinement factors are calculated for TM modes with the transfer matrix method (TMM) and effective index method (EIM). The thicknesses of the cladding layer and waveguide layer, the ridge-width, and the cavity length are all taken into account. Appropriate thicknesses of epilayers are given with lower threshold gain and more economical material growth time.

**Key words:** quantum cascade laser; transfer matrix method; effective index method

**PACC:** 4260B; 7850G

**CLC number:** TN365

**Document code:** A

**Article ID:** 0253-4177(2007)01-0031-05

## 1 Introduction

The quantum cascade laser (QCL), invented at Bell Laboratory in 1994<sup>[1]</sup>, is a promising light source in the mid-infrared range. Great achievements have been made<sup>[2~4]</sup> in the past few years. Continuous wave operation at room temperature of InP-based QCLs and pulsed room temperature operation of GaAs-based QCLs have been reported. Although GaAs/AlGaAs QCLs have the potential for flexible design due to good lattice matching over the entire alloy composition, one of the critical problems limiting the performance of GaAs-based QCLs is the thick cladding layers. Thus, optimizing the waveguide structure, which can reduce losses, improve the confinement factors, and thereby reduce the threshold, is a feasible way to enhance device performances.

There are several initial considerations in the design of waveguides for GaAs-based QCLs. To get a higher confinement factor, a greater index contrast between the active region and cladding layers is necessary to reduce the leak of modes. However, due to the considerable extinction coefficients (imaginary part of the refractive index)

of the cladding layers, the waveguide losses must be decreased by separating the active region from the cladding layers by waveguide layers, which are normally comprised of low-doped GaAs. In the early design of GaAs-based QCLs, AlGaAs was used as the material of the cladding layers<sup>[5]</sup> because it has a higher index than the active region. However, in AlGaAs layers, variations of the ionized carrier concentrations produce strong instabilities in device thresholds and slope efficiencies. In addition, the growth of thick AlGaAs layers is difficult due to residual strain. The main problem is that AlGaAs layers have poorer electrical and thermal conductivity than the GaAs layers. Therefore, Al-free cladding layers have been adopted. Most recently, heavily-doped GaAs has been used as the material of cladding layers. The heavily-doped GaAs layers decrease the refractive index and shift the plasma frequency of the cladding layers close to that of the lasers<sup>[6]</sup>. Due to the plasma resonance, the real part of the refractive index dramatically decreases, but the extinction coefficient also increases. It seems that enhancing the optical confinement is incompatible with decreasing the waveguide losses. Besides the effect of epilayer thickness, the width of the ridge is an

\* Project supported by the National Science Fund for Distinguished Young Scholars (No. 60525406), the National Natural Science Foundation of China (Nos. 90101002, 60136010), the State Key Development Program for Basic Research of China (No. G20000683-2), and the National High Technology Research and Development Program of China (Nos. 2001AA311140, 2005AA31G040)

<sup>†</sup> Corresponding author. Email: fqliu@red.semi.ac.cn

Received 24 May 2006, revised manuscript received 22 August 2006

©2007 Chinese Institute of Electronics

important parameter of lasers that also plays an important role in improving device performance.

In this paper, modal losses and confinement factors are calculated for different thicknesses of waveguide and cladding layers with the transfer matrix method (TMM). The appropriate thicknesses of epilayers are recommended that yield lower losses and a higher confinement factor, and simultaneously shorten the growth time. The effect of different ridge widths is then taken into consideration by the effective index method (EIM) with the recommended structure. In our calculation, material losses are represented by the imaginary part of the refractive index.

## 2 Theory and methodology

### 2.1 TMM and EIM

For analyzing the mode profile of a 1D multi-layer slab waveguide, the well known TMM, which requires little computational power, is an efficient method. In the calculation, only TM modes are taken into account because of the intersubband lasing nature of the QCL. When the influence of the ridge width is introduced, the EIM<sup>[8]</sup> is applied at the same time, in the following manner. As shown in Fig. 1(a), the rib waveguide is first divided into three regions, each of which can be represented as a 1D slab optical waveguide. For each 1D waveguide, the effective index along the  $x$  axis is calculated by TMM. A slab waveguide is then modeled by placing the effective indices calculated in the former step along the  $y$  axis (See Fig. 1(b)). Eventually the effective index is obtained by

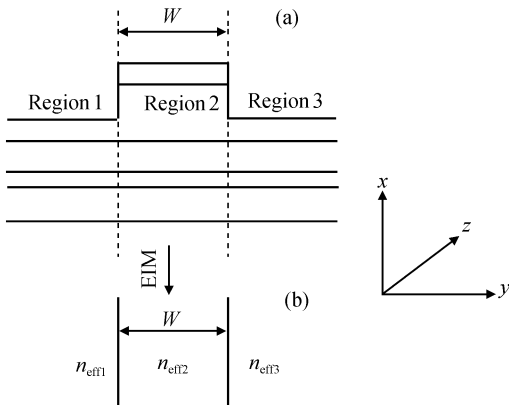


Fig. 1 Concept of the effective index method

solving the model with TMM once again, but assuming TE polarized modes ( $y$  direction). In the calculation only the base mode is considered because it is predominant in all modes.

### 2.2 Waveguide model

When the effect of epilayer thickness is considered, we use a simplified slab structure in our calculation, as shown in Fig. 2. The cladding layer, waveguide layer, and substrate are all made of GaAs, and the doping concentrations are  $6 \times 10^{18}$ ,  $4 \times 10^{16}$ , and  $2 \times 10^{18} \text{ cm}^{-3}$ , respectively. The active region consists of 30 periods, the detailed structure of which is described in Ref. [9], and the injector layers are doped to  $6 \times 10^{17} \text{ cm}^{-3}$ . The complex permittivity is obtained by using the Drude model, which gives us

$$\epsilon = \epsilon_b + i \frac{ne^2\tau}{\omega m^* (1 - i\omega\tau)} \quad (1)$$

where  $\omega$  is the angular frequency of the radiation,  $\epsilon_b$  the relative (free-space) dielectric constant,  $n$  the carrier concentration,  $e$  the elementary charge,  $m^*$  the effective electron mass, and  $\tau$  the momentum relaxation time. For these simulations,  $\epsilon_b$  is set at 12.4 and  $m^*$  is set at  $0.067m_0$  for GaAs. The Drude relaxation times for GaAs used in this paper are 100fs for the highly doped (cladding) layers, 500fs for the lightly doped (waveguide) layers, and 300fs for the medium doped (injector) layers<sup>[10,11]</sup>. The parameters for the Au contact layer are taken as  $\tau = 21\text{ps}$  and  $\epsilon_b = 8$ ,  $n = 5.9 \times 10^{22} \text{ cm}^{-3}$  and  $m^* = m_0$ <sup>[12]</sup>. The refractive index of  $\text{SiO}_2$  used is given in Ref. [13].

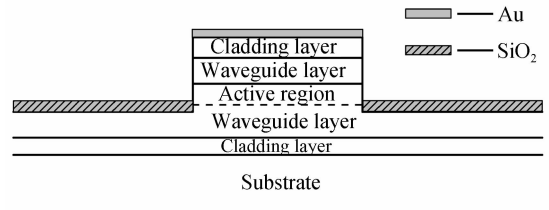


Fig. 2 Simplified model of QCL ridge waveguide structure

### 2.3 Threshold gain

For the comparison of different waveguide structures, we use the threshold gain  $g_{th}$  as a figure-of-merit, which is given by

$$g_{th} = \frac{\alpha_w + \alpha_m}{\Gamma} = \frac{2\text{Im}(\beta) - \ln(R)/L}{\Gamma} \quad (2)$$

where  $\alpha_w = 2\text{Im}(\beta)$  is the absorptive loss contributed by the waveguide, and  $\beta$ , the propagation constant of the base mode in the QCL, is determined by  $\beta = \frac{2\pi n_{\text{eff}}}{\lambda}$ , with  $n_{\text{eff}}$  being the effective refractive index of the mode;  $\alpha_m = -\ln(R)/L$  is the mirror loss,  $L$  is the cavity length,  $R$  is the facet reflectivity which for a GaAs/air interface is normally  $\sim 0.32$ <sup>[10]</sup>; and  $\Gamma$  is the confinement factor. All the parameters except  $\alpha_m$  on the right side of Eq. (2) are determined by the passive waveguide structure. Since lower threshold gain is more propitious to the reduced threshold current density and increased operating temperature, better device performances may be achieved with waveguide optimization to reduce the threshold gain.

### 3 Results

#### 3.1 Thickness variation of waveguide layer

First, the thickness of the cladding layers  $L_c$  is fixed, and the various thicknesses of the waveguide layer  $L_w$  are investigated. In the calculation, infinite (1D) and finite ridge widths are considered. For the case in which the thickness of the cladding layers is  $1\mu\text{m}$  and the cavity length is  $1\text{mm}$ , the plot of the threshold gain versus the thickness of the waveguide layer is shown in Fig. 3. The lowest threshold gain occurs at a waveguide layer thickness of  $2.5\mu\text{m}$ . For detailed discussion, the effects of  $\alpha_w/\Gamma$  and  $\alpha_m/\Gamma$  for 1D analysis, as an example, are shown in the inset of Fig. 3. The data for the 2D case differ insignificantly from the 1D case. The waveguide layer thickness dramatically influences the waveguide loss and confinement factor. A thicker waveguide layer will keep the active region away from the heavily-doped cladding layer and yield a much lower waveguide loss, although this is accompanied by a decrease in the confinement factor as the mode overlaps the thicker waveguide layer more. Thus the term  $\alpha_w/\Gamma$  decreases as the waveguide layer thickness increases. However, since the facet loss  $\alpha_m$  is nearly independent of the waveguide structure, the  $\alpha_m/\Gamma$  term begins to blow up with increasing waveguide layer thickness as the confinement degrades. Therefore, at a certain thickness of waveguide layer, the minimal thresh-

old gain can be found.

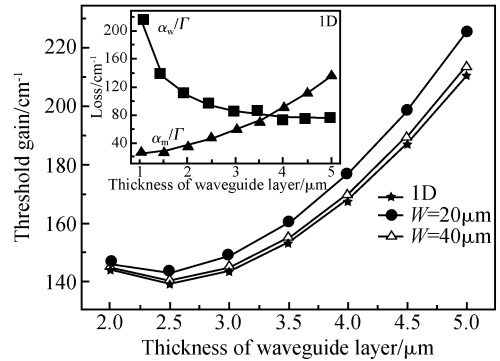


Fig. 3 Threshold gain versus the thickness of waveguide layer for a constant cladding layer of  $1\mu\text{m}$  and cavity length of  $1\text{mm}$ . The 1D condition and finite ridge widths of  $20\mu\text{m}$  and  $40\mu\text{m}$  are considered. The inset is the contribution from the waveguide and mirror losses to the threshold gain as the waveguide layer thickness increases in 1D.

#### 3.2 Thickness variation of cladding layer

With the same cavity length as above and waveguide layer thickness of  $2.5\mu\text{m}$ , the results of threshold gain versus thickness of cladding layer are shown in Fig. 4. Whatever the ridge width, the threshold gain decreases as the cladding layer thickness increases. However, after the thickness  $L_c$  exceeds  $1.4\mu\text{m}$ , the rate of decrease slows gradually. More details can be obtained in 1D analysis as an example as shown in the inset of Fig. 4. Due to the large contrast between the indexes of the waveguide and cladding layers, the mode will be limited effectively in the active re-

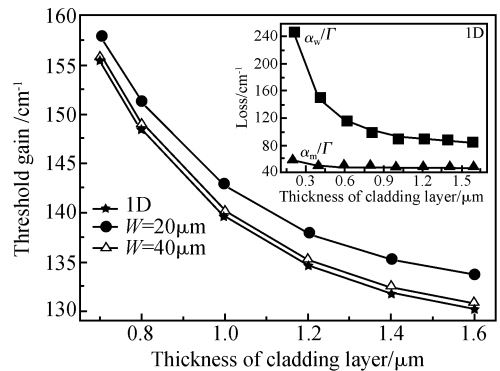


Fig. 4 Threshold gain versus the thickness of cladding layer for a constant waveguide layer of  $2.5\mu\text{m}$  and cavity length of  $1\text{mm}$ . The 1D condition and the finite ridge widths of  $20\mu\text{m}$  and  $40\mu\text{m}$  are considered. The inset is the contribution from the waveguide and mirror losses to the threshold gain as the cladding layer thickness increases in 1D.

gion. A thicker cladding layer will result in a higher confinement factor, while at the same time the waveguide loss will decrease as the mode overlaps the lossy heavily-doped cladding layer less. However, the mode limit is not directly proportional to the thickness of the cladding layer, and less and less modal intensity is pushed into the active region as the cladding layer thickness increases sequentially, thus slowing the increase of the confinement factor. Therefore, although the terms  $\alpha_w/\Gamma$  and  $\alpha_m/\Gamma$  both decrease with increasing cladding layer thickness, they change little for very thick cladding layers. Because of the difficulties of long-period material growth, uninterruptedly increasing the thickness of the cladding layer merely to get a slightly lower threshold gain is not feasible. From the above analysis, we highly recommend a cladding layer thickness of  $1.4\mu\text{m}$ .

### 3.3 Variation of cavity length

Finally, the effect of cavity length is considered. As indicated by Eq. (2), the variation of cavity length only affects the mirror loss  $\alpha_m$ . From the above discussion, the mirror loss is nearly constant as the thickness of the cladding layer changes, but it plays an important role in the contribution to the threshold gain while altering the waveguide layer thickness. Thus only the variation of the waveguide layer thickness is considered in the calculation. For the case in which the ridge width is  $20\mu\text{m}$  and the thickness of the cladding layer is fixed at  $1.4\mu\text{m}$  as recommended above, the result is shown in Fig. 5. The trend of threshold gain is almost the same when the cavity length increases from 1 to 3mm. However, the lowest threshold

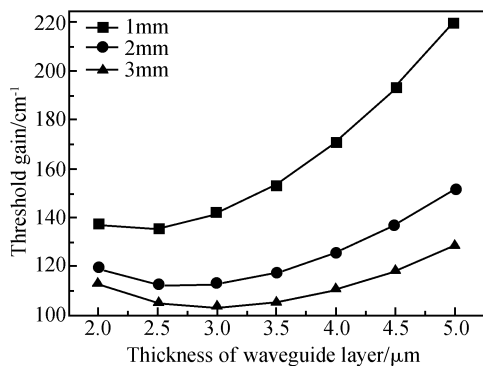


Fig.5 Threshold gain versus cavity length for a constant cladding layer thickness of  $1.4\mu\text{m}$  and ridge width of  $20\mu\text{m}$

gain is displayed at a waveguide layer thickness of  $3\mu\text{m}$  when the cavity length is 2 or 3mm, which is different from the case in which the cavity length is 1mm. Since the cavity length is mainly selected to be  $1\sim 3\text{mm}$  in device fabrication, the value of the waveguide layer thickness should be reconfirmed to be some value between  $2.5\sim 3\mu\text{m}$ .

## 4 Conclusion

Using the TMM and EIM, we have calculated the losses and confinement factors of the base mode for a  $9.0\mu\text{m}$  GaAs-based QCL structure. In addition to the waveguide thicknesses, the ridge width and cavity length are all involved in our calculation. The results indicate that a structure with waveguide layer thickness of  $2.5\sim 3\mu\text{m}$  and cladding layer thickness of  $1.4\mu\text{m}$  is optimal for lowering the threshold gain, and simultaneously economizes the period of material growth.

## References

- [1] Faist J, Capasso F, Sivco D L, et al. Quantum cascade lasers. *Science*, 1994, 264(22): 553
- [2] Liu F Q, Zhang Y Z, Zhang Q S, et al. Room temperature operation of strain-compensated quantum cascade lasers. *Electron Lett*, 2000, 36(20): 1704
- [3] Yu J S, Evans A, David J, et al. High-power continuous-wave operation of quantum-cascade lasers up to  $60^\circ\text{C}$ . *IEEE Photonics Technol Lett*, 2004, 16(9): 747
- [4] Liu Fengqi, Zhang Yongzhao, Zhang Quansheng, et al. Strain-compensated InGaAs/InAlAs quantum cascade laser. *Chinese Journal of Semiconductors*, 2000, 21(10): 1038 (in Chinese) [刘峰奇, 张永照, 张权生, 等. 应变补偿 InGaAs/InAlAs 量子级联激光器. *半导体学报*, 2000, 21(10): 1038]
- [5] Sirtori C, Kruck P, Barbieri S, et al. GaAs/Al<sub>x</sub>Ga<sub>1-x</sub>As quantum cascade lasers. *Appl Phys Lett*, 1998, 73(24): 3486
- [6] Sirtori C, Kruck P, Barbieri S, et al. Low-loss Al-free waveguides for unipolar semiconductor lasers. *Appl Phys Lett*, 1999, 75(25): 3911
- [7] Borges B V, Romero M A, Cesar A C. An extension of the effective index method to analyze leakage losses in rib type waveguides. *Inter J Infrar Milli Wave*, 1999, 20(10): 1783
- [8] Kawano K, Kitoh T. *Introduction to optical waveguide analysis*. New York: John Wiley & Sons, 2001
- [9] Page H, Becker C, Robertson A, et al. 300K operation of a GaAs-based quantum-cascade laser at  $\lambda \approx 9\mu\text{m}$ . *Appl Phys Lett*, 2001, 78(22): 3529
- [10] Kohen S, Williams B S, Hu Q. Electromagnetic modeling of terahertz quantum cascade laser waveguides and resonators. *J Appl Phys*, 2005, 97(5): 053106-1
- [11] Indjin D, Ikonc Z, Harrison P, et al. Surface plasmon waveguides with gradually doped or NiAl intermetallic compound buried contact for terahertz quantum cascade lasers. *J Appl Phys*, 2003, 94(5): 3249

- [12] Sachs R, Roskos H G. Mode calculations for a terahertz quantum cascade laser. *Optics Express*, 2004, 12(10):2062
- [13] Palik E D. Handbook of optical constants of solids. Orlando: Academic FL, 1985

## 9.0 $\mu\text{m}$ GaAs 基量子级联激光器的波导优化\*

李 路 刘峰奇<sup>†</sup> 邵 烨 刘俊岐 王占国

(中国科学院半导体研究所 材料科学重点实验室, 北京 100083)

**摘要:** 通过转移矩阵法和有效折射率法计算了 9.0 $\mu\text{m}$  GaAs 基量子级联激光器波导的模式损耗和限制因子, 从而对其波导结构进行优化. 计算中考虑了各外延层的厚度、脊宽和腔长的影响. 给出了在较低阈值下节约材料生长时间的各外延层厚度.

**关键词:** 量子级联激光器; 转移矩阵法; 有效折射率法

**PACC:** 4260B; 7850G

**中图分类号:** TN365

**文献标识码:** A

**文章编号:** 0253-4177(2007)01-0031-05

\* 国家杰出青年科学基金(批准号:60525406), 国家自然科学基金(批准号:90101002, 60136010), 国家重点基础研究发展规划(批准号:G20000683-2)以及国际高技术研究发展计划(批准号:2001AA311140 和 2005AA31G040)资助项目

<sup>†</sup> 通信作者. Email: fqliu@red.semi.ac.cn

2006-05-24 收到, 2006-08-22 定稿